

Article

# Assessment of Changes in Water Balance Components under 1.5 °C and 2.0 °C Global Warming in Transitional Climate Basin by Multi-RCPs and Multi-GCMs Approach

Ying Hao <sup>1,2,3</sup>, Jingjin Ma <sup>4</sup>, Jing Chen <sup>5</sup>, Dongyong Wang <sup>3</sup>, Yuan Wang <sup>1,\*</sup> and Hongmei Xu <sup>6,\*</sup>

<sup>1</sup> School of Atmospheric Sciences, Nanjing University, Nanjing 210023, China; dg1328006@smail.nju.edu.cn

<sup>2</sup> Meteorological Center of Huaihe Basin, Anhui Meteorological Bureau, Hefei 230031, China

<sup>3</sup> Anhui Meteorological Observatory, Anhui Meteorological Bureau, Hefei 230031, China; amo\_wangdongyong@163.com

<sup>4</sup> Beijing Meteorological Disaster Prevention Center, Beijing Meteorological Bureau, Beijing 100089, China; majingjin@126.com

<sup>5</sup> Tianjin Institute of Meteorological Science, Tianjin Meteorological Bureau, Tianjin 300074, China; cjl1\_1@163.com

<sup>6</sup> National Climate Center, China Meteorological Administration, Beijing 100081, China

\* Correspondence: yuanasm@nju.edu.cn (Y.W.); xuhm@cma.gov.cn (H.X.); Tel.: +86-138-5172-9795 (Y.W.); +86-136-2118-6170 (H.X.)

Received: 25 November 2018; Accepted: 12 December 2018; Published: 15 December 2018



**Abstract:** The global warming of 1.5 °C and 2.0 °C proposed in the Paris Agreement has become the iconic threshold of climate change impact research. This study aims to assess the potential impact of 1.5 °C and 2.0 °C global warming on water balance components (WBC) in a transitional climate basin—Chaobai River Basin (CRB)—which is the main water supply source of Beijing. A semi-distributed hydrological model SWAT (Soil and Water Assessment Tool) was driven by climate projections from five General Circulation Models (GCMs) under three Representative Concentration Pathways (RCPs) to simulate the future WBC in CRB under the 1.5 °C and 2.0 °C global warming, respectively. The impacts on annual, monthly WBC were assessed and the uncertainty associated with GCMs and RCPs were analyzed quantitatively, based on the model results. Finally, spatial variation of WBC change trend and its possible cause were discussed. The analysis results indicate that all the annual WBC and water budget are projected to increase under both warming scenarios. Change trend of WBC shows significant seasonal and spatial inhomogeneity. The frequency of flood will increase in flood season, while the probability of drought in autumn and March is expected to rise. The uneven spatial distribution of change trend might be attributed to topography and land use. The comparison between two warming scenarios indicates that the increment of 0.5 °C could lead to the decrease in annual surface runoff, lateral flow, percolation, and the increase in annual precipitation and evapotranspiration (ET). Uncertainties of surface runoff, lateral flow, and percolation projections are greater than those of other components. The additional 0.5 °C global warming will lead to larger uncertainties of future temperature, precipitation, surface runoff, and ET assessment, but slightly smaller uncertainties of lateral flow and percolation assessment. GCMs are proved to be the main factors that are responsible for the impact uncertainty of the majority assessed components.

**Keywords:** water balance components; RCPs; GCMs; assessment; 1.5 °C and 2.0 °C global warming

## 1. Introduction

Global warming is one of the greatest climate issues that human beings face. The latest researches of Intergovernmental Panel on Climate Change (IPCC) Fifth Assessment Report Working Group I [1] showed that global mean surface temperature (GMT) has increased 0.85 °C over the period of 1880–2012 and will likely increase 0.3 °C to 0.7 °C in the near-term. Due to the changes in various meteorological elements, global warming has the potential to significantly alter hydrologic cycle and influence river flow regimes consequently [2–5]. An additional threat is also posed to water security as a result of significant changes in water supply in many regions. Therefore, in the interest for effective water resource management and planning, impact assessment of the future climate change on the hydrological response is crucial [6–9], especially for water-scarce areas.

Recent studies [10–13] have used physically-based distributed hydrological models (HMs) driven by General Circulation Models (GCMs) to understand the impact of climate change on hydrological process on the basin scale. In addition, the uncertainties in impact assessments were also explored and discussed [14–17]. From the previous research, the main factors that are responsible for the uncertainty were concluded as follows: Scenarios of economic development, greenhouse gas emission scenarios and aerosol emissions scenarios, GCM, downscaling technique, the hydrological model structure and parameterization. Among these main factors, the uncertainties associated with GCMs are the largest source of impact uncertainty on the global scale. However, the dominant factors which contribute to the largest degree of uncertainty vary across climate regions. Therefore, multiple combinations of GCMs and emission scenarios should be used to assess the regional hydrological response to climate change [18]. After RCPs were proposed by IPCC AR5 in 2014, researches on the hydrology and water resource prediction has also been carried out using the new scenario [19,20].

The 2015 Paris Agreement set out a global action plan that includes two long-term temperature goals. One is to avoid dangerous climate changes by limiting global average temperature increase to well below 2.0 °C above pre-industrial levels, and the other is pursuing efforts towards a target of 1.5 °C for a sustainable future. On 8 October 2018, the IPCC special report on global warming at 1.5 °C has been released in Incheon, South Korea. The report assesses the climate impact under global warming of 1.5 °C and 2.0 °C and points out that the global warming of 1.5 °C is likely to reach as soon as 2030. Thus far, 1.5 °C and 2.0 °C has become the iconic threshold and has been used as a politically useful marker for global scale mitigation strategies. The evaluation of climate change impacts at warming of 1.5 °C and 2 °C was first provided by Schlessner et al. in 2016 [21] on the global scale along with many similar studies [22,23].

As discussed before, the changes of the hydrological cycle caused by the temperature increase and its corresponding uncertainties are regionally dependent [24]. Therefore, in order to make the global warming of 1.5 °C and 2.0 °C a helpful metric to provide reliable information for regional adaptation policies, climate impacts should be projected on regional scales. CRB is located on the transitional climate region where the climate ranges from semi-arid to sub-humid [25]. The topography, land use, and soil type, as well as weather condition of CRB have great spatial variability, which will influence the response of the hydrological cycle to climate change [26]. Due to the complexity of this issue and limited data, few researches have been conducted and the understanding of hydrological cycle response under 1.5 °C and 2.0 °C global warming in this transitional climate basin is still incomplete. Nevertheless, the impact assessment is of utmost importance for CRB, which provides two-thirds of fresh water resource for Beijing, the capital of China. Therefore, assessment of climate change effect on WBC, which can reflect water resources more comprehensively than the river runoff is of great significance in CRB under 1.5 °C and 2.0 °C global warming. During the past few years, most researches mainly focused on river discharge response [21–23], the potential effect of global warming on water balance components was relatively less explored. Recently, the possible changes in WBC in many regions and basins under different global warming scenarios have been studied. Most of them were based on SRES (Special Report on Emissions Scenarios) scenarios proposed by AR4 (the 4th Assessment Report) [27–30]. There are only few researches use the latest released RCPs [31,32],

and even fewer researches focused on the impact of 1.5 °C and 2.0 °C global warming. Similar to the results in the river discharge [19,22,23], change trends of water balance components also vary from regions and exhibit uncertainties associated with scenarios and GCMs.

This study focused on the following issues, can a hydrological model be applied in a transitional climate basin for water balance analysis? How different are WBC projections from different GCMs and RCPs and which is the main source of uncertainty? What are the future possible changes of WBC to climate forcing under 1.5 °C and 2 °C global warming in CRB?

The issues were addressed in three steps in this study:

- (1) Evaluate the applicability of the SWAT model for ET as well as discharge simulations in the CRB;
- (2) The difference and uncertainties of projected impacts associated with GCMs structure and RCPs scenarios were estimated and compared quantitatively;
- (3) Assess the impact of 1.5 °C and 2 °C global warming on WBC by multi-GCMs and multi-RCPs approach. The differences of the impact between 1.5 °C and 2.0 °C global warming was highlighted. Besides, the possible effects of topography, land use and soil type on WBC change were analyzed.

## 2. Materials and Methods

### 2.1. Study Area

The CRB with the catchment area of 13846 km<sup>2</sup> is located in the northern part of North China plain (115°25' E~117°45' E, 39°10' N~41°40' N). It originated from Yanshan Mountain and pass through Hebei, Beijing, and Tianjin provinces with the total length of 458 km. Chaobai River basin consists of two major tributaries, Chao River and Bai River, which converge into Miyun Reservoir in the downstream. CRB is characterized by complex topography, mountainous area, and alluvial plain constitute 87% and 13% of the basin, respectively. The CRB featuring semi-humid semiarid climate regime has four distinctive seasons, that is, cold and dry in winter and hot and rainy in summer. The annual mean temperature and precipitation are 9.11°C and 559.3 mm, respectively. However, precipitation has uneven seasonal distribution and concentrated in flood season (June to September) accounts for 80.2% of annual rainfall.

### 2.2. Data

#### 2.2.1. Geographic Data of CRB

The SWAT model was built up based on the following geographic data:

- Digital elevation model (DEM) with a scale of 1:50,000 obtained from the national database of China Fundamental Geographic Information Center.
- The soil property data used herein provided by Harmonized World Soil Database by Food and Agriculture Organization (<http://www.fao.org/>).
- Land use data with resolution of 1 km from the Environmental and Ecological Science Data Center for West China (<http://westdc.westgis.ac.cn>). Due to limited data, changes of land use were not considered in the WBC simulation during reference period and in the future.

#### 2.2.2. Hydrological Data

Hydrological observations used for calibration and validation of the SWAT model were collected from the Water Year Book of Haihe Basin. The measured monthly discharges at the Zhangjiafen hydrological gauge along Bai River and the Xiahui hydrological gauge along Chao River during 1961–1990 were available for calibration, and data during 1991–2001 was utilized for validation.

### 2.2.3. Meteorological Data

Daily precipitation and temperature data at  $0.5^\circ$  resolution for the period of 1958 to 2001 was derived from WATCH reanalysis data according to the European Water and Global Change Project and used as climate forcing ([http://www.eu-watch.org/data\\_availability](http://www.eu-watch.org/data_availability)). In order to assess the quality of WATCH data over CRB, long-term (1961–2001) precipitation and temperature observations from two meteorological stations (Fengning and Miyun) were used to calculate correlation coefficient ( $r$ ). Results show that  $r$  of annual mean precipitation, annual mean maximum temperature, and minimum temperature at Fengning and Miyun are 0.99/0.81, 0.85/0.88, and 0.85/0.86, respectively, which indicates that WATCH data is reliable in the CRB and has good potential to be used as an alternative data to drive hydrological model [33,34]. The locations of the meteorological observation stations and the grid points of the WATCH reanalysis are shown in Figure 1. In order to evaluate the simulation performance of SWAT for ET, Global monthly land surface evapotranspiration (ET) data with a spatial resolution of  $1.0^\circ \times 1.0^\circ$  from 1983 to 2001 were obtained from NASA Hydrology and Earth System Science Fellowship programs (<http://www.ntsg.umt.edu/project/global-et.php>). The research results of Zhang et al. showed that the monthly ET estimates are in favorable agreement with observations (RMSE = 13.0–15.3 mm month<sup>-1</sup>;  $R^2 = 0.80$ –0.84) from globally representative land cover types. Besides, the estimated global ET capture observed spatial and temporal variations at basin-scale (RMSE = 186.3 mm·yr<sup>-1</sup>;  $R^2 = 0.80$ ) as well as the global scale. Despite the uncertainties of ET calculations associated with tower eddy flux measurements and remote sensed NDVI, this long-term global ET record can be used for climate change assessment of terrestrial water with well-quantified accuracy [35,36].

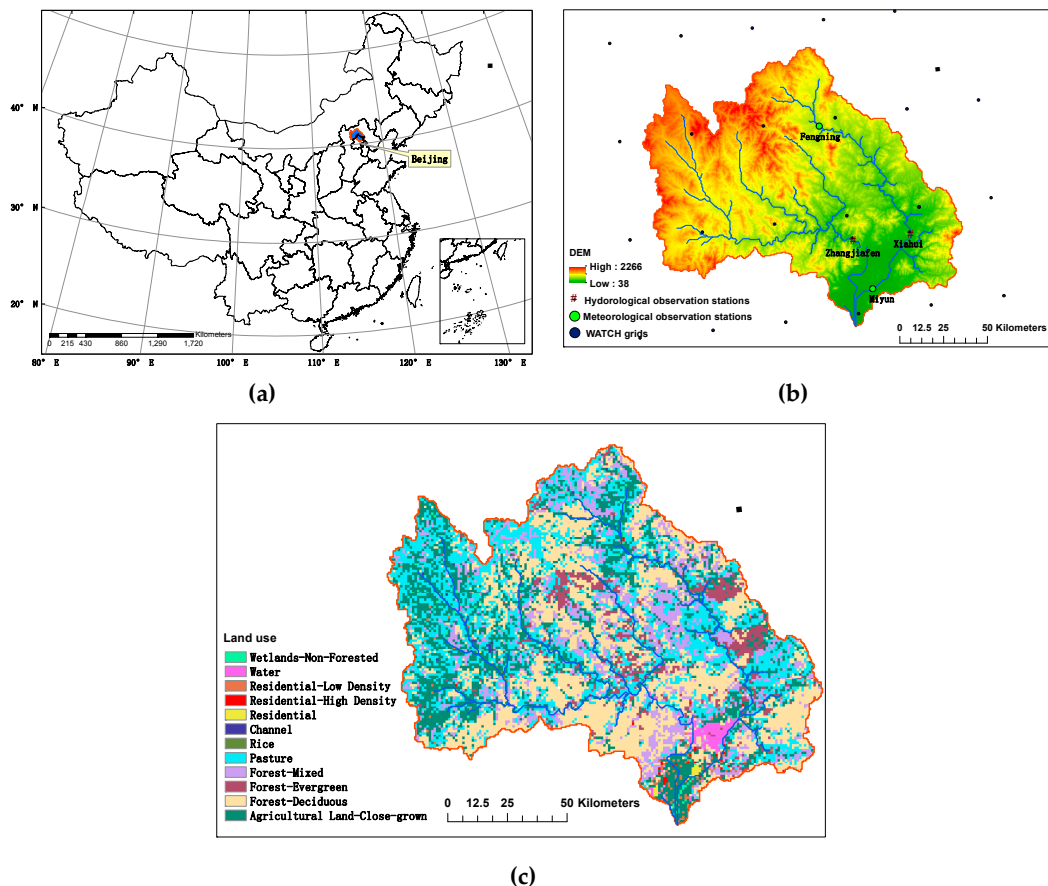


**Figure 1.** (a) Location of the CRB in China; (b) overview map of the CRB, DEM (shade), hydrological gauges (triangles), meteorological stations (green circles), and grid notes of climate forcing (black dots); and (c) the land use of the CRB.

#### 2.2.4. Climate Projections

Climate projections from five GCMs (GFDL-ESM2M, HaDGem2, IPSL\_CM5A\_LR, MIROC-ESM-CHEM, NorESM1-M, abbreviated as GFDL, HAD, IPSL, MIROC, and NOR, respectively) of the CMIP5 project in the framework of ISIMIP [37–39] under three Representative Concentration Pathways (RCP4.5, RCP6.0, and RCP8.5) were used to drive the SWAT model for future projection. The FRC index (Fractional range coverage) of the five GCMs in ISI-MIP project is 0.75 and 0.59, respectively, which is better than the five GCMs randomly selected from CMIP5, and can reasonably represent the changes of regional average temperature and precipitation [38]. The climate dataset provide daily projected precipitation and temperature data covering the period from 1950 to 2099. The aforementioned climate projections data were bias corrected using trend-preserving bias correction approach and downscaled to  $0.5^\circ \times 0.5^\circ$  resolution to match with WATCH's resolution [13,40].

In this study, a baseline period from 1986 to 2005, which is consistent with Schlessner, C.F. et al. [21] was selected to compare with the projections. The GMT during the baseline period is  $0.61^\circ\text{C}$  warmer than preindustrial levels (1850–1900) [1]. Therefore, the warming of  $0.89^\circ\text{C}$  and  $1.39^\circ\text{C}$  above reference period correspond to the commonly accepted threshold of  $1.5^\circ\text{C}$  and  $2^\circ\text{C}$  above preindustrial, respectively.

### 2.3. Methodology

#### 2.3.1. Climate Change Scenarios

The combination of 5 GCMs and 3 RCPs produces 15 climate change scenarios (referred to as the GCM-RCP combination hereafter). The 30 years moving averaged surface temperatures of the 15 scenarios were calculated and compared with the baseline to specify the future time horizon that surpasses  $1.5^\circ\text{C}$  and  $2.0^\circ\text{C}$  global warming. The results indicated that the projected GMT of all scenarios surpass the warming of  $1.5^\circ\text{C}$  above pre-industrial level, while 14 out of 15 scenarios surpass the threshold of  $2.0^\circ\text{C}$ .

#### 2.3.2. Soil and Water Assessment Tool (SWAT) Model

SWAT is a semi-distributed, physically-based hydrological model developed by United States Department of Agriculture for long-term continuous watershed scale simulation [41]. The model integrates the state-of-the-art of remote sensing (RS), geographic information system (GIS), and digital elevation model (DEM) technologies and is able to simulate the water cycle with a high level of spatial detail. SWAT was widely applied on medium to large scale basins to assess the impact of management measure and climate change on hydrological processes, agricultural chemical yield, and sediment [42–45]. The water cycle simulated by SWAT is based on water balance equation which includes precipitation, surface runoff, lateral flow, actual evapotranspiration, percolation, baseflow, and change of soil water content [42]. In CRB, the annual mean value of the aforementioned WBC during reference period are 489.59, 21.08, 15.06, 437.22, 25.03, 7.81, and 0.48 mm, respectively. Change of soil water content and baseflow are much smaller than other variables, so five water balance components (precipitation, surface runoff, lateral flow, ET, and percolation) were selected for this study. The runoff that flows laterally within the soil body is called lateral flow. Percolation is the amount of water that percolates past the root zone during the time step.

In this study, the latest SWAT version, that is ArcGIS compatible ArcSWAT2012 [46] was used for assessment. The CRB was divided into 64 sub-basins based on DEM and 363 hydrological response units were further sub-divided according to soil type, land use and slope class. The Penman-Monteith method [47] was used to calculate the evapotranspiration. The improved Soil Conservation Service Curve Number (SCS-CN) method [48] was used to estimate the surface runoff, and the Muskingum method [49] was applied to calculate the river course.

### 2.3.3. Model Calibration and Validation

The WATCH dataset from 1958 to 2001 were used to drive the SWAT model. The 44 years data were split into three periods according to their usages in SWAT, the warming-up period (1958–1960), the calibration period (1961–1990) and the validation period (1991–2001). In order to evaluate the performance of water balance components simulation, both discharge observations (1961–2001) and the global monthly ET data (1983–2001) were used to calibrate and validate the SWAT model. Prior to calibration, a Latin Hypercube one-at-a-time (LH-OAT) technique, proposed by Morris [50], and implemented in SWAT-CUP (SWAT Calibration and Uncertainty Programs) was applied to investigate the sensitivity of parameters [51]. Sequential Uncertainty Fitting (SUFI2) algorithm in SWAT-CUP generic interface was applied for automatic calibration and parameter optimization [51]. To make the evaluation statistics robust, multiple criteria for goodness-of-fit, namely coefficient of determination ( $R^2$ ), Nash-Sutcliff efficiency coefficient (NSE) [52], and percentage of bias (PBIAS) were selected to quantify the performance of SWAT model by comparing monthly modeling results with in-situ observations. In general, the model simulation is considered acceptable when the  $R^2$  and NSE values are greater than 0.5.

### 2.3.4. Hydrological Projections

Projected annual and monthly mean surface runoff, lateral flow, percolation, and ET in the CRB were simulated by SWAT driven by 15 climate change scenarios. Changes in annual mean temperature and WBC at the two warming levels are presented by the percentage change relative to the baseline. As the small value of WBC in winter during baseline period may lead to abnormally large percentage change, so absolute change is used for monthly WBC analysis. Aridity index (AI) [53] and water budget (WB) were also calculated to assess the degree of water deficiency quantitatively in CRB. In order to quantify projection uncertainty, standard deviation (SD) was used to measure the dispersion of different GCMs and RCPs prediction results

$$AI = P/PET \quad (1)$$

where P is the average annual precipitation (mm), PET is the average annual potential evapotranspiration (mm). AI is further divided into 5 levels, hyper-arid ( $AI < 0.05$ ), arid ( $0.05 < AI < 0.2$ ), semi-arid ( $0.2 < AI < 0.5$ ), dry sub-humid ( $0.5 < AI < 0.65$ ) and humid ( $AI > 0.65$ ) regions, that means the larger the AI, the humid the region.

$$WB = P - ET \quad (2)$$

where P is the average precipitation (mm), ET is the average evapotranspiration (mm).

## 3. Results

### 3.1. Sensitivity Analysis

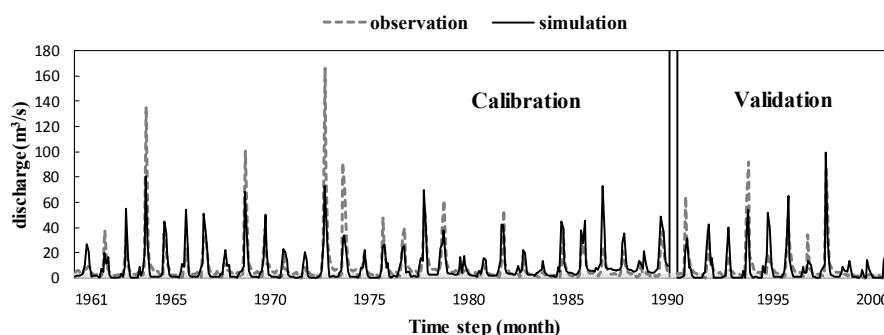
Table 1 shows the sensitivity analysis of SWAT model parameters. Generally, ESCO, HRU\_SLP, SOL\_K, CN2, CANMX, SOL\_AWC, and SLSUBSN which show larger absolute values of t-statistics and smaller p-values (surpass 5% level of significance) are the most sensitive parameters for the basin. Soil evaporation compensation factor (ESCO) that is related with the main hydrologic processes of evapotranspiration is the most sensitive parameter. HRU\_SLP, SOL\_K and SOL\_AWC are particularly sensitive due to their effect on lateral flow [30,54]. This should be expected because 87% of the catchment is mountainous area with higher lateral flow contribution. As the primary parameter for runoff yield, the SCS curve number at moisture condition II (CN2) is found to be the 4th ranked critical parameter. Maximum canopy storage (CANMX) ranks the 5th sensitive parameter. This could be partly explained by high coverage of forest in CRB.

**Table 1.** SWAT parameter sensitivity to monthly discharge in CRB.

Parameter	Description	Unit	T-Stat	p-Value
ESCO	Soil evaporation compensation factor		21.285	0.000
HRU_SLP	Average slope steepness		−9.535	0.000
SOL_K	Soil hydraulic conductivity	mm·h <sup>−1</sup>	−8.739	0.000
CN2	Curve number for moisture condition II		−7.838	0.000
CANMX	Maximum canopy storage	mm	7.263	0.000
SOL_AWC	Soil water available capacity		6.417	0.000
SLSUBBSN	Average slope length		2.490	0.013
GWQMN	Minimum depth for groundwater flow occurrence	mm	1.867	0.063
ALPHA_BF	Baseflow alpha factor	Day <sup>−1</sup>	−1.052	0.293
CH_N2	Manning's roughness coefficient		0.884	0.377
GW_DELAY	Groundwater delay	day	−0.712	0.477
SOL_Z	Soil depth	mm	0.363	0.716

### 3.2. SWAT Performance Evaluation

The comparison between the simulated and measured flow duration curves indicates that the SWAT model well captures the inner and inter-annual variations of the observed discharge at both Xiahui (Figure 2) and Zhangjiafen (Figure 3) stations. However, SWAT always underestimates peak discharge. The various evaluation statistics during the calibration and validation periods are listed in Table 2. During the calibration period (1961–1990), the simulated monthly discharge at Xiahui station along the Chao River correlates well with the corresponding observed records with a  $R^2$  value of 0.68, NSE values of 0.67, a PBIAS value of 11.8%. The performance of SWAT at the Zhangjiafen station along the Bai River is similar with a  $R^2$  value of 0.71, a NSE value of 0.66, a PBIAS value of 31.7%. During the validation period, the observed and simulated discharge show good agreement with  $R^2$  of 0.70 (0.71), NSE of 0.50 (0.51), and PBIAS of 5.8% (13.6%) at the Xiahui (Zhangjiafen) station. There was good agreement between remote sensing based and simulated ET duration curves (Figure 4). Calibration and validation results of the ET at CRB were proved to be quite satisfactory. During calibration (validation) period, the values of  $R^2$ , NSE and PBIAS are 0.90 (0.84), 0.87 (0.69), and 12.5% (8.8%), respectively. Both SWAT simulated and remote sensed annual mean ET decline from East to West and show similar spatial pattern. However, simulated ET exhibits more inhomogeneous with the probable cause of land use (Figure 5)

**Figure 2.** Monthly observed and simulated discharge at Xiahui station along Chao River.**Table 2.** The results of statistical evaluation indices during calibration and validation at Xiahui station along Chao River and Zhangjiafen station along Bai River.

Tributary	Hydrological Station	Catchment Area/km <sup>2</sup>	Calibration			Validation		
			R <sup>2</sup>	NSE	PBIAS	R <sup>2</sup>	NSE	PBIAS
Chao River	Xiahui	6960.6	0.68	0.67	11.8%	0.70	0.50	5.8%
Bai River	Zhangjiafen	8827.4	0.71	0.66	31.7%	0.71	0.51	13.6%

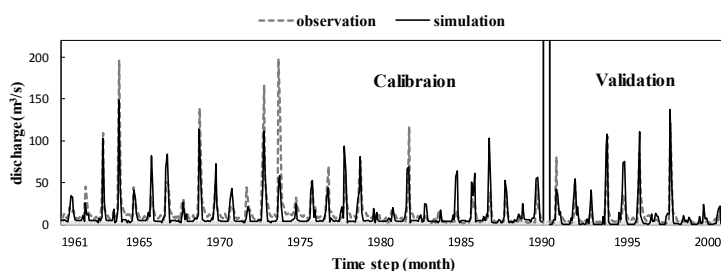


**Figure 3.** Monthly observed and simulated discharge at Zhangjiafen station along Bai River.

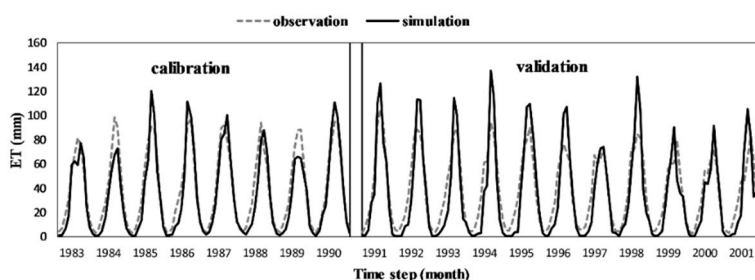


**Figure 4.** The monthly observed and simulated ET (Evapotranspiration) at CRB (Chaobai River Basin) during calibration and validation periods.

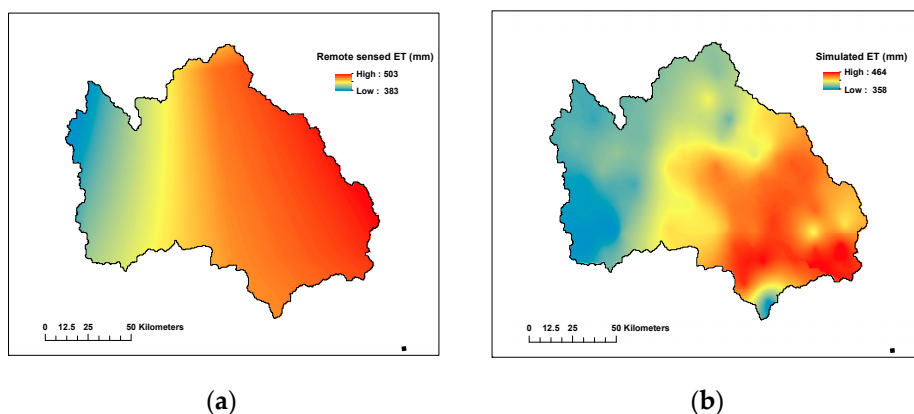


**Figure 5.** The spatial distribution of the annual mean ET during 1983–2006. (a) Remote sensed; (b) SWAT simulated.

### 3.3. Changes in Annual mean Temperature

In summary, the statistics illustrated that the historical WBC in CRB can be reproduced with an acceptable accuracy and ensured the successful application of SWAT model for climate change impact assessment in this study.

The annual mean temperature of the GCM-RCP combination in CRB is expected to increase by 1.3 °C and 2.0 °C under global warming of 1.5 °C and 2.0 °C relative to the baseline, respectively. As we mentioned before, the global mean temperature in the baseline period is 0.61 °C warmer than pre-industrial, which means that the projected annual mean temperature in CRB is 1.91 °C and 2.61 °C warmer than pre-industrial level for two warming levels. However, the increase of annual mean temperature differs among GCMs and RCPs. The lowest (highest) increase is 1.04 °C and 1.62 °C (1.52 °C and 2.50 °C) for 1.5 °C and 2.0 °C global warming, respectively. Among the five GCMs, the NOR and MIROC show the highest increase and HAD has the smallest increase (Table 3). The variation of projected change in annual mean temperature among different RCPs is smaller with a value of 1.27–1.30 °C (1.97–2.01 °C) for 1.5 °C (2.0 °C) global warming.

**Table 3.** Changes in annual mean temperature in CRB under the 1.5 °C and 2.0 °C global warming (°C).

Global Warming	RCP	GFDL	HAD	IPSL	MIROC	NOR	Mean GCMs
1.5 °C	4.5	1.51	1.06	1.23	1.39	1.33	1.30
	6	1.27	1.11	1.05	1.53	1.43	1.28
	8.5	1.04	1.04	1.25	1.47	1.52	1.27
	Mean RCPs	1.27	1.07	1.18	1.46	1.43	1.28
2.0 °C	4.5	*	1.62	1.82	2.07	2.50	2.00
	6	1.93	1.64	1.68	2.39	2.20	1.97
	8.5	1.77	1.65	1.95	2.31	2.37	2.01
	Mean RCPs	1.85	1.63	1.82	2.26	2.36	1.99

\* Indicates that the change in global mean surface temperature projected by GFDL under RCP4.5 will not surpass the threshold of 2 °C.

The uncertainty of annual mean temperature projection in the GCM-RCP combination is accessed by its SD. The GCM-RCP combination has a SD of 0.18 °C and 0.30 °C under two global warming scenarios, respectively, which implies that the increment of 0.5 °C could lead to larger uncertainty. The SDs among different GCMs is 2.0 and 3.3 times against that of different RCPs for the 1.5 °C and 2.0 °C warming level, respectively. This result indicates that different GCMs are the main source of uncertainty.

### 3.4. Changes in Water Balance Components

#### 3.4.1. Annual Water Balance

The annual mean precipitation anomalies of the GCM-RCP combination relative to preindustrial baseline (1986–2005 mean) over CRB are shown in Figure 6. The annual mean precipitation is projected to increase by 5.3% and 7.1% under 1.5 °C and 2.0 °C global warming, respectively. However, the directions and magnitudes of projected changes differ from GCMs and RCPs. GFDL projected the most significant increasing tendency of annual precipitation (11.1%/13.7% under two warming scenarios, respectively), followed by IPSL which showed increases of 7.8% and 13.0%. MIROC and NOR, which ranked third and fourth, also projected an evident increasing trend. Contrary to the aforementioned four GCMs, HAD projected a decrease tendency with the magnitude of -2.8% and -2.2% at two warming levels, respectively. For all three RCPs, the increasing tendencies were projected under two warming scenarios and the magnitudes of change increase with the temperature except for RCP8.5.

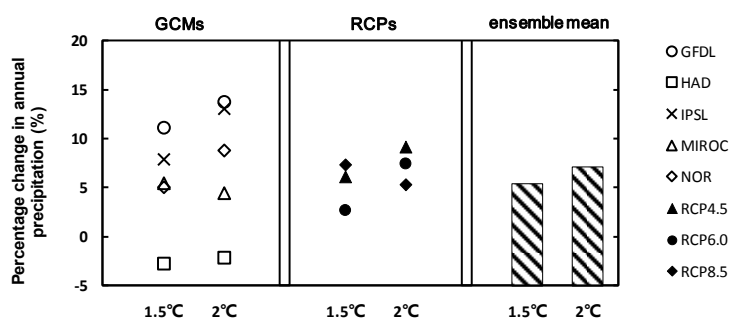


**Figure 6.** Percentage change in annual mean precipitation in CRB.

The SDs of annual mean precipitation among the whole ensemble are 6.9% and 7.1% for the 1.5 °C and 2.0 °C warming scenarios. The GCMs are still the main source of uncertainty with SDs among different GCMs 1.4 and 2.0 times larger than those among different RCPs for the 1.5 °C and 2.0 °C warming period, respectively.

Percentage changes of annual mean surface runoff, lateral flow, percolation, and ET refer to baseline are shown in Figure 7. The ensemble mean results indicate that the annual mean surface

runoff, lateral flow, percolation, and ET in CRB will increase by 25.8%, 19.9%, 29.0%, and 2.5%, respectively, compared to the baseline for the 1.5 °C warming scenarios. Under the 2.0 °C global warming, the annual mean surface runoff, lateral flow, and percolation are projected to increase by smaller amplitudes with an average of 23.3%, 18.3%, and 23.8%, respectively. However, the increasing tendency of the projected annual mean ET become more dramatic with an average of 4.7% than that for 1.5 °C warming. The results imply that the additional 0.5 °C increase could lead to a decrease in the annual surface runoff, lateral flow, percolation, and increase in the annual ET. The water budget is projected to increase by 15.8 mm (13.1 mm) under the 1.5 °C (2.0 °C) warming scenario. The mean arid index (AI) of GCM-RCP combination is 0.54 at the 1.5 °C warming level, which is 0.01 higher than baseline. When at the 2.0 °C warming level, the AI is 0.001 higher than baseline. The above analysis indicate that the CRB may become wetter under both warming scenarios, especially under global warming of 1.5 °C.

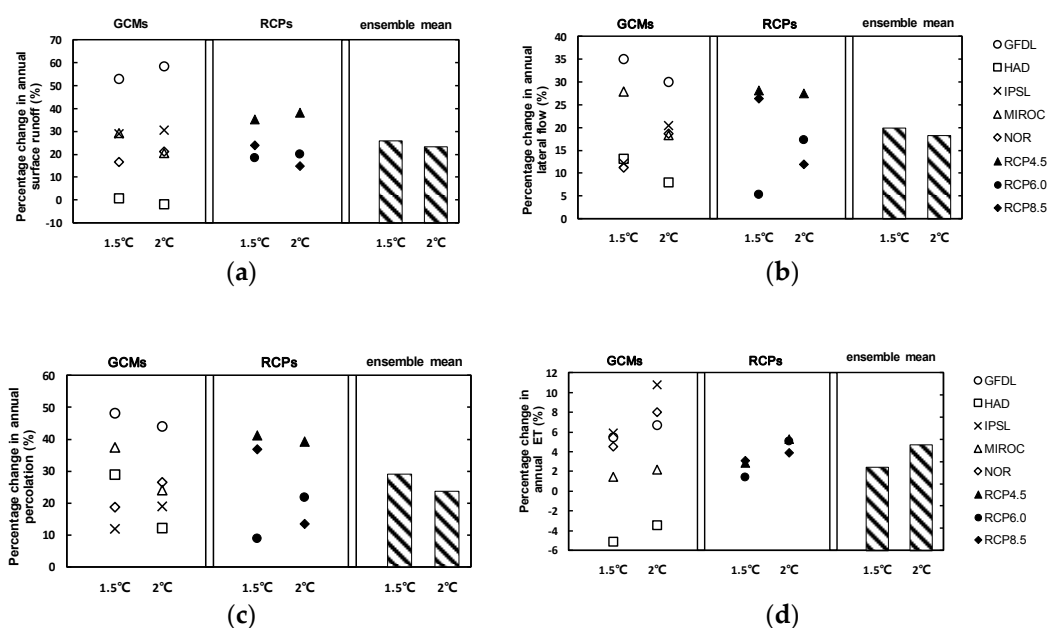


**Figure 7.** Percentage change in annual surface runoff (a), annual lateral flow (b), annual percolation (c), and annual ET (d) under 1.5 °C and 2 °C global warming in CRB.

The magnitudes and directions of changes in WBC generated from the five GCMs are different from one another. Under the 1.5 °C warming scenario, the changes of surface runoff driven by the five GCMs has large variation, ranging from 0.9% (HAD) to 53.0% (GFDL). Under the 2.0 °C warming scenario, the increase tendency of surface runoff modeled by GFDL is still the largest (58.4%), while HAD projected a slightly negative tendency (−1.9%). The increase rates projected by other three GCMs under 2.0 °C global warming vary from 20.3% (MIROC) to 30.4% (IPSL). The changes in the lateral flow range from 11.2% (NOR) to 35.1% (GFDL) under 1.5 °C warming and from 7.9% (HAD) to 30.1% (GFDL) under 2.0 °C warming, respectively, which is relatively smaller than those in the surface runoff. For percentage changes in the annual mean percolation, projections driven by GFDL under 1.5 °C warming scenario still show the maximum increase rate (48.1%), while IPSL shows the minimum increase rate (11.9%). Under the 2.0 °C warming scenario, the increase tendencies of annual percolation range from 12.2% (HAD) to 44.1% (GFDL). Compared with the aforementioned four water balance components, the variation of annual mean ET projected by five GCMs was the smallest, ranging from -5.0% (HAD) to 5.9% (IPSL) under the 1.5 °C global warming and from -3.5% (HAD) to 10.8% (IPSL) under the 2.0 °C global warming.

Generally, all the three RCPs agree on an increase tendency of change in WBC in CRB. However, the magnitudes under three RCPs are different from one another. For the global warming of 1.5 °C,

the WBC shows a significant increase under RCP4.5 and RCP8.5, while the results projected under RCP6.0 shows a relatively smaller increase. For the global warming of 2.0 °C, the projections of WBC under RCP4.5 are still proved to have the maximum increase rate, followed by RCP6.0, the simulations under RCP8.5 show the minimum increase rate.

The SD of percentage changes of GCM-RCP combination in surface runoff, lateral flow, and percolation are 26.1%, 25.6%, and 20.5%, respectively, under the 1.5 °C warming, which implies a considerable uncertainty. Uncertainty in the ET projection is relatively smaller with a SD of 4.6%. For the global warming of 2.0 °C the uncertainty of the surface runoff and ET projections is slightly larger than that under the 1.5 °C warming with SDs of 27.3% and 5.5%, respectively. Nevertheless, the uncertainty of lateral flow and percolation projections decrease slightly. For the changes in the surface runoff and ET, the GCMs are the main source of uncertainty for the climate change impact. Uncertainty associated with different GCMs is 2.4/2.0 (surface runoff) and 5.6/8.4 (ET) times larger than those with different RCPs for 1.5 °C and 2.0 °C warming levels, respectively. For the projected lateral flow and percolation, the uncertainty from GCMs is similar to that from RCPs for two warming scenarios.

### 3.4.2. Monthly Water Balance

The box-whisker plots (Figures 8–12) show change in monthly mean WBC forced by five GCMs under three RCPs under 1.5 °C and 2.0 °C global warming, respectively. Generally, the largest changes are observed for the ET, which implies the high sensitivity of ET to rainfall and temperature inputs. Meanwhile, the monthly change of lateral flow under two warming scenarios show the smallest difference in reference to baseline.

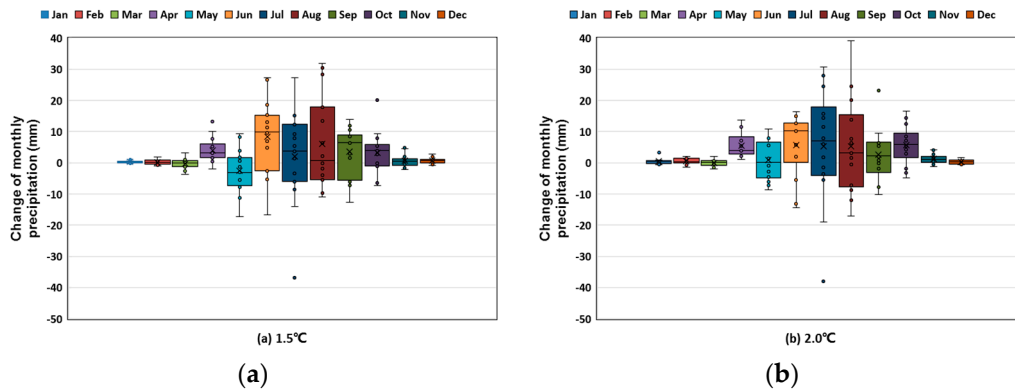


Figure 8. Change of monthly precipitation refer to baseline period (a) 1.5 °C; (b) 2.0 °C.

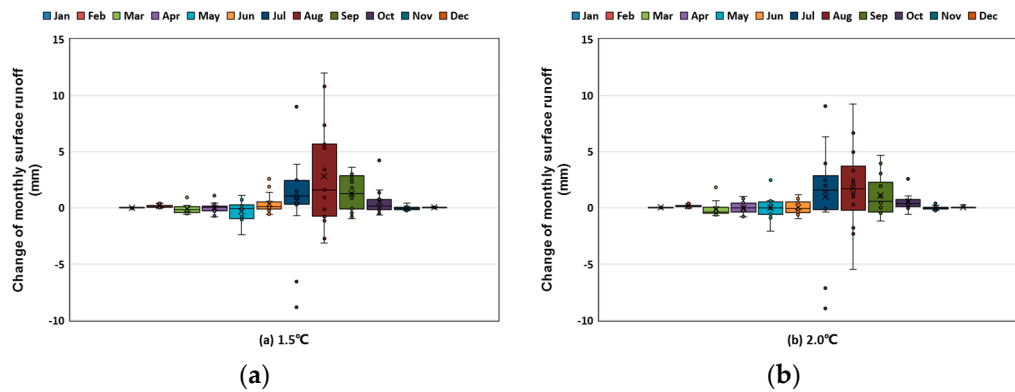


Figure 9. Change of monthly surface runoff refer to baseline period (a) 1.5 °C; (b) 2.0 °C.

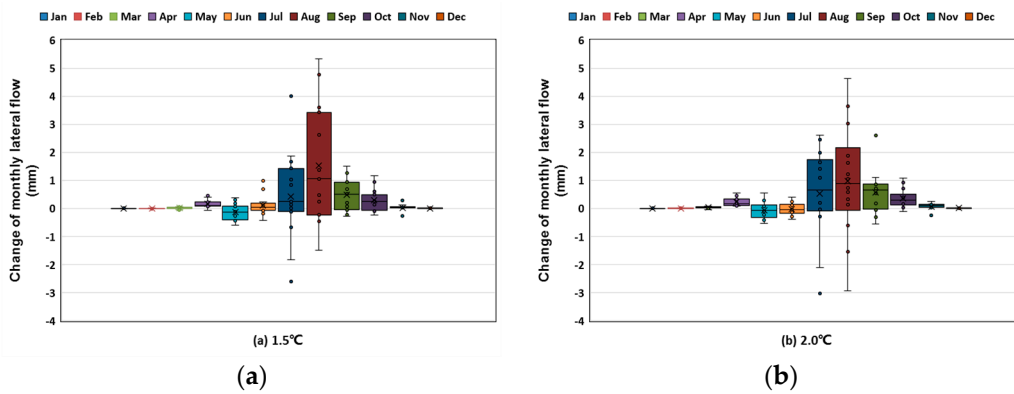


Figure 10. Change of monthly lateral flow refer to baseline period (a) 1.5 °C; (b) 2.0 °C.

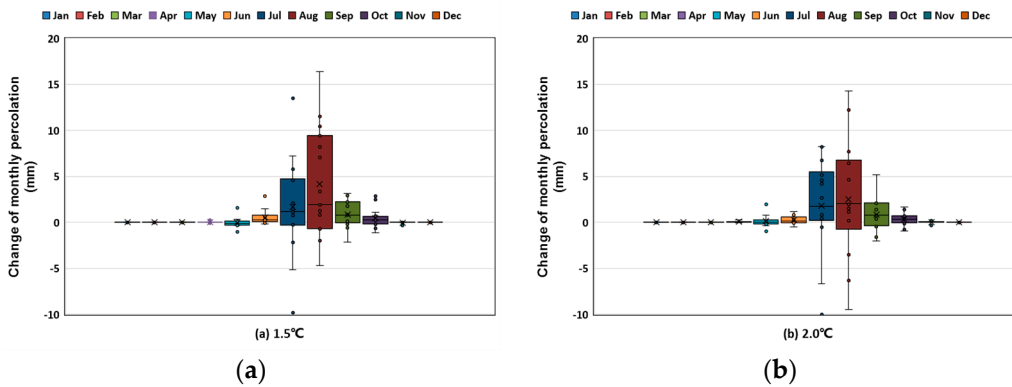


Figure 11. Change of monthly percolation refer to baseline period (a) 1.5 °C; (b) 2.0 °C.

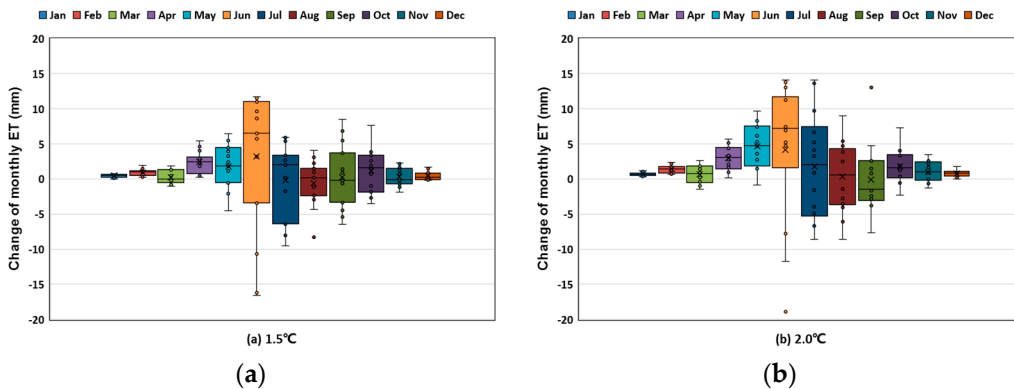
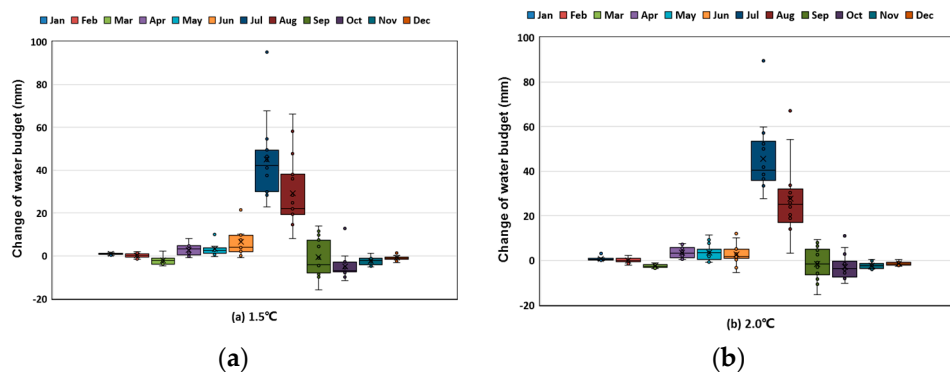


Figure 12. Change of monthly ET refer to baseline period (a) 1.5 °C; (b) 2.0 °C.

In summer and early autumn (from June to October), the monthly mean precipitation is projected to increase significantly. However, surface runoff, later flow and percolation will only increase significantly between July and September which is flood season. This could be related to a pronounced positive change in June and little or negative change from July to September for the ET component. It should be noted that the most significant increases of surface runoff, lateral flow, and percolation are observed in August.

The water budget shows a slight increase from April to June and a significant increase from July to August under both global warming scenarios (Figure 13). The largest positive change in water budget is observed in July with an average of 43.6 mm (45.7 mm) at 1.5 °C (2.0 °C) warming level. In autumn and March, water budget exhibits slightly negative change at both warming levels. The above observations imply that frequency and strength of flood during flood season is likely to increase. Meanwhile, the probability of drought occurrence is expected to increase in autumn and

March in CRB. Generally, the change magnitudes of WBC under 1.5 °C warming scenario will be larger than those under 2.0 °C warming scenario.



**Figure 13.** Monthly water budget under global warming scenarios (a) 1.5 °C; (b) 2.0 °C.

GCMs were proved to be the main source of uncertainty for all the five water balance components. The uncertainty of WBC monthly change associated with GCMs is 2.0~4.1, 1.7~3.8 times larger than those with RCPs under 1.5 °C and 2.0 °C global warming, respectively. Additionally, among five water balance components, projected results of monthly change in precipitation show the largest variation between different GCMs and RCPs, followed by ET. The simulated monthly change in lateral flow is proved to have the smallest uncertainty with the average deviation of 0.45 mm under both global warming periods. The uncertainty in summer and autumn is much larger than that in spring and winter.

#### 4. Discussion

It is found that the change trends of WBC under global warming feature uneven spatial distribution in this transitional climate basin. Figures 14 and 15 show that the percentage changes of annual precipitation and ET are larger in mountainous area (Northwest) and smaller in alluvial plain (Southeast) under both two warming scenarios. However, spatial distribution of percentage change in surface runoff, lateral flow and percolation has no obvious relation with topography (not shown). In order to find out the potential causes for the spatial inhomogeneity of change in WBC, the correlation coefficients of WBC percentage change and proportion of land use, soil type in 65 sub-basins were calculated, respectively. The result (Table 4) indicates that deciduous forest always show significant positive tendency of lateral flow, surface runoff, and percolation under both 1.5 °C and 2.0 °C global warming, while pasture has lower increasing tendency. Under 1.5 °C global warming, the effect of land use on the change of abovementioned three components is more apparent than that under 2.0 °C global warming. The annual surface runoff at mixed forest and ET at agriculture land are expected to increase by smaller amplitudes under 2.0 °C global warming.

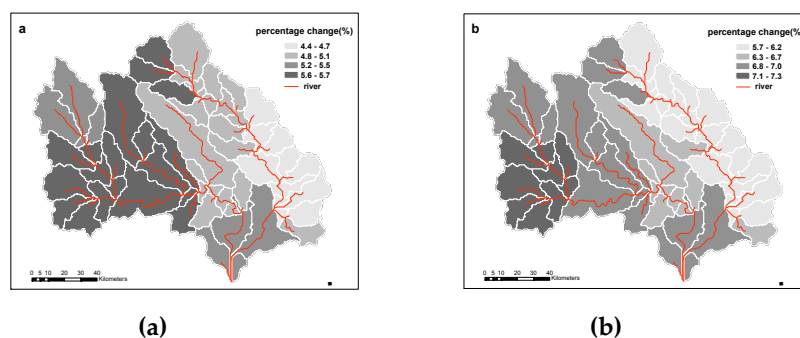


**Figure 14.** Spatial distribution of precipitation percentage changes under (a) 1.5 °C; (b) 2.0 °C warming scenarios.

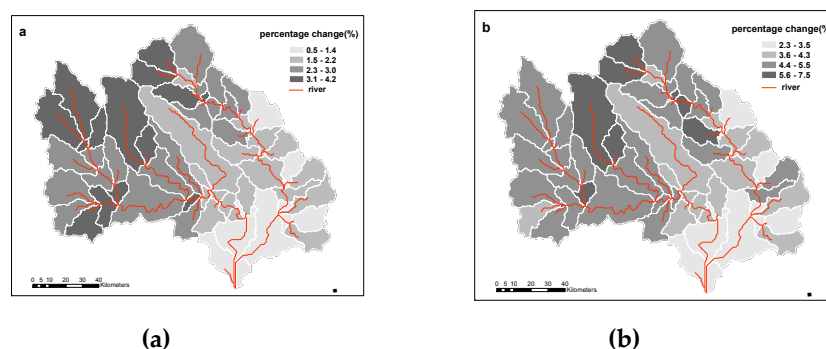


**Figure 15.** Spatial distribution of annual ET percentage changes under (a) 1.5 °C, (b) 2.0 °C global warming.

**Table 4.** Correlation coefficient of percentage change in WBC and land use, soil type.

Factors	Detailed Classification	Surface Runoff (1.5 °C/2.0 °C)	Lateral Flow (1.5 °C/2.0 °C)	Percolation (1.5 °C/2.0 °C)	ET (1.5 °C/2.0 °C)
land use	Agriculture land	−0.10/0.14	−0.25/−0.07	−0.25/−0.13	−0.29/−0.34 *
	Deciduous Forest	0.63 */0.37 *	0.44 */0.21	0.51 */0.38 *	0.17/0.15
	Pasture	−0.35 */−0.35 *	−0.47 */−0.36 *	−0.41 */−0.35 *	0.04/0.21
	Mixed Forest	−0.19/−0.35 *	−0.16/−0.25	−0.16/−0.25	0.24/0.27
Soil type	luvisol	0.20/−0.09	0.03/−0.24	0.14/−0.11	0.23/0.33 *
	Semi-luvisol	−0.05/0.19	0.04/0.23	0.02/0.20	−0.11/−0.23
	Calcicsols	−0.23/−0.13	−0.09/0.02	0.19/0.22	0.23/0.11
	Initial develop soil	0.00/−0.02	−0.01/−0.01	−0.06/−0.05	0.15/0.12
	semi-hydromorphic soil	−0.07/−0.10	−0.12/−0.11	−0.25/−0.24	−0.23/−0.13

\* Illustrates r passed the significant test at 0.01 level.

Generally, compared with land use, soil type has little impact on change trend of WBC. However, when the soil type is luvisol, ET shows more significant increase, especially under the 2.0 °C warming scenario.

Responses of WBC to climate change are influenced by many factors, except for topography, land use and soil type. Our study can reach some preliminary conclusions as follows. Topography and land use might be factors that have an important impact to increasing magnitude of WBC. Percentage changes of annual precipitation and ET are larger in mountainous area and smaller in alluvial plain under both two warming periods. Deciduous forest always show significant positive tendency of lateral flow, surface runoff and percolation under both 1.5 °C and 2.0 °C global warming, while pasture has lower increasing tendency. Generally, soil type has little impact on change trend of WBC.

## 5. Conclusions

The WATCH data during 1961 to 2001 was utilized to drive the SWAT model and the simulation results were compared with the observed monthly discharge and remote sensing based ET during the calibration and validation periods. The results show that the historical stream flow and ET in the CRB can be reproduced with an acceptable accuracy and ensured the successful application of SWAT model for climate change impact assessment in this study. The future possible hydrological responses to climate forcing was assessed quantitatively under three RCPs for 1.5 °C and 2 °C global warming scenarios. The main conclusions are as follows.

- (1) The annual mean temperatures of GCM-RCP combination are projected to increase by 1.3 °C and 2.0 °C respectively for global warming of 1.5 °C and 2 °C relative to the baseline. All the water balance components in CRB are expected to increase under both warming scenario. The additional 0.5 °C increase could make decrease in annual surface runoff, lateral flow, percolation, water budget, and increase in precipitation, ET. CRB will become wetter under 1.5 °C warming scenario than under 2.0 °C warming scenario. However, the change does not have apparent effect on arid index.

- (2) Projected changes in monthly water balance illustrate that the significant increase trend of surface runoff, lateral flow in flood season will lead to more flood events in CRB. CRB is likely to face more droughts in autumn and March due to the decrease of water budget. The magnitudes of WBC monthly change are larger under 1.5 °C warming scenario than those under 2.0 °C warming scenario.
- (3) Generally, compared with land use, soil type has little impact on change trend of WBC. However, when the soil type is luvisol, increasing trend of ET will be more significant, especially under 2.0 °C global warming.
- (4) Generally, the increase tendencies of WBC modeled by GFDL and IPSL are the largest, while HAD projected the lowest positive or slightly negative tendency for two warming scenarios. Contrast to GCMs, almost all projected annual temperature, precipitation and WBC under three RCPs agree on a positive tendency under both two global warming scenarios. The WBC simulation results projected under RCP4.5 show higher increase amplitudes, while the relative lower increase amplitudes are projected under RCP8.5 and RCP6.0.
- (5) Quantitative uncertainty analysis indicated that, although the additional 0.5 °C global warming will lead to larger uncertainties of most WBC assessment, but the gap of uncertainty between two warming scenarios is not significant. The results also showed that comparing with the uncertainty of ET and precipitation projection, uncertainties of surface runoff, lateral flow, and percolation projection are much greater. GCMs were proved to be the most important contributor to uncertainty of majority assessed components in both warming scenarios with the exception of percolation and lateral flow. Therefore, the selection of climate forcing input is of vital importance.

**Author Contributions:** Conceptualization, Y.W. and H.X.; Data curation, J.C.; Formal analysis, J.M. and J.C.; Funding acquisition, Y.W.; Methodology, Y.H. and D.W.; Resources, J.M.; Software, Y.H.; Validation, Y.H.; Writing—original draft, Y.H.; Writing—review & editing, Y.W. and H.X.

**Funding:** This research was funded by The National Key R&D Program of China (2016YFE0102400) and climatic change project of the China Meteorological Administration (CCSF201810).

**Acknowledgments:** The authors thank Xiaowen Tang for his helpful comments on the manuscript. Data from five GCMs were obtained from Inter-Sectoral Impact Model Intercomparison Project (ISIMIP) (<https://esg-pik-potsdam.de>).

**Conflicts of Interest:** The authors declare no conflict of interest.

## References

1. IPCC. *Climate Change 2013: The Physical Science Basis. Contribution of Working Group I to the Fifth Assessment Report of the Intergovernmental Panel on Climate Change*; Cambridge University Press: Cambridge, MA, USA, 2013.
2. Chang, H.; Moradkhani, H.; Jung, I.W. Quantifying uncertainty in urban flooding analysis considering hydro-climatic projection and urban development effects. *Hydrol. Earth Syst. Sci.* **2011**, *15*, 617–633.
3. Wang, Q.F.; Wu, J.J.; Lei, T.J.; He, B.; Wu, Z.; Liu, M.; Mo, X.Y.; Geng, G.P.; Li, X.H.; Zhou, H.K.; et al. Temporal-spatial characteristics of severe drought events and their impact on agriculture on a global scale. *Quat. Int.* **2014**, *349*, 10–21. [[CrossRef](#)]
4. Duan, L.L.; Cai, T.J. Changes in magnitude and timing of high flows in large rain-dominated watersheds in the cold region of north-eastern China. *Water* **2018**, *10*, 1658. [[CrossRef](#)]
5. Li, B.; Chen, F.; Guo, H.D. Regional complexity in trends of potential evapotranspiration and its driving factors in the Upper Mekong River basin. *Quat. Int.* **2015**, *380*, 83–94. [[CrossRef](#)]
6. Schnorbus, M.A.; Cannon, A.J. Statistical emulation of streamflow projections from a distributed hydrological model: Application to CMIP3 and CMIP5 climate projections for British Columbia, Canada. *Water Resour. Res.* **2014**, *50*, 8907–8926. [[CrossRef](#)]
7. Lyu, J.Q.; Shen, B.; Li, H.E. Dynamics of major hydro-climatic variables in the headwater catchment of the Tarim River Basin, Xinjiang, China. *Quat. Int.* **2015**, *380*, 143–148. [[CrossRef](#)]

8. Wu, F.F.; Wang, X.; Cai, Y.P.; Li, C.H. Spatiotemporal analysis of precipitation trends under climate change in the upper reach of Mekong River basin. *Quat. Int.* **2016**, *392*, 137–146. [[CrossRef](#)]
9. Bai, P.; Liu, X.M.; Liang, K.; Liu, C.M. Investigation of changes in the annual maximum flood in the Yellow River basin, China. *Quat. Int.* **2016**, *392*, 168–177. [[CrossRef](#)]
10. Khoi, D.N.; Suetsugi, T. Impact of climate and land-use changes on hydrological processes and sediment yield—A case study of the Be River catchment, Vietnam. *J. Hydrol. Sci.* **2014**, *59*, 1095–1108. [[CrossRef](#)]
11. Huang, Z.H.; Xue, B.; Pang, Y. Simulation on stream flow and nutrient loadings in Gucheng Lake, Low Yangtze river basin, based on SWAT model. *Quat. Int.* **2009**, *208*, 109–115. [[CrossRef](#)]
12. Alfieri, L.; Burek, P.; Feyen, L.; Forzieri, G. Global warming increases the frequency of river floods in Europe. *Hydrol. Earth Syst. Sci.* **2015**, *19*, 2247–2260. [[CrossRef](#)]
13. Vetter, T.; Huang, S.; Aich, V.; Yang, T.; Wang, X.; Krysanova, V.; Hattermann, F. Multi-model climate impact assessment and intercomparison for three largescale river basins on three continents. *Earth Syst. Dyn.* **2015**, *6*, 17–43. [[CrossRef](#)]
14. Bastola, S.; Murphy, C.; Sweeney, J. The role of hydrological modeling uncertainties in climate change impact assessments of Irish river catchments. *Adv. Water Resour.* **2011**, *34*, 562–576. [[CrossRef](#)]
15. Najafi, M.R.; Moradkhani, H.; Jung, I.W. Assessing the uncertainties of hydrologic model selection in climate change impact studies. *Hydrol. Process.* **2011**, *25*, 2814–2826. [[CrossRef](#)]
16. Hagemann, S.; Chen, C.; Clark, D.B.; Folwell, S.; Gosling, S.N.; Haddeland, I.; Hanasaki, N.; Heinke, J.; Ludwig, F.; Wiltshire, A.J. Climate change impact on available water resources obtained using multiple global climate and hydrology models. *Earth Syst. Dyn.* **2013**, *4*, 129–144. [[CrossRef](#)]
17. Dams, J.; Nossent, J.; Senbeta, T.B.; Willems, P.; Batelaan, O. Multi model approach to assess the impact of climate change on runoff. *J. Hydrol.* **2015**, *529*, 1601–1616. [[CrossRef](#)]
18. Braud, I.; Roux, H.; Anquetin, S.; Maubourguet, M.M.; Manus, C.; Viallet, P.; Dartus, D. The use of distributed hydrological models for the Gard 2002 flash flood event: Analysis of associated hydrological processes. *J. Hydrol.* **2010**, *394*, 162–181. [[CrossRef](#)]
19. Su, B.; Huang, J.; Zeng, X.; Jiang, T. Impacts of climate change on streamflow in the upper Yangtze River basin. *Clim. Chang.* **2017**, *141*, 1–14. [[CrossRef](#)]
20. Shrestha, S.; Bach, T.V.; Pandey, V.P. Climate change impacts on groundwater resources in Mekong Delta under representative concentration pathways (RCPs) scenarios. *Environ. Sci. Policy* **2016**, *61*, 1–13. [[CrossRef](#)]
21. Schleussner, C.F.; Lissner, T.K.; Fischer, E.M. Differential climate impacts for policy-relevant limits to global warming: The case of 1.5 °C and 2 °C. *Earth Syst. Dyn.* **2016**, *7*, 327–351. [[CrossRef](#)]
22. Liu, L.L.; Xu, H.M.; Wang, Y.; Jiang, T. Impacts of 1.5 and 2 °C global warming on water availability and extreme hydrological events in Yiluo and Beijiang River catchments in China. *Clim. Chang.* **2017**, *145*, 145–158. [[CrossRef](#)]
23. Chen, J.; Gao, C.; Zeng, X.F.; Su, B. Assessing changes of river discharge under global warming of 1.5 °C and 2 °C in the upper reaches of the Yangtze River Basin: Approach by using multiple- GCMs and hydrological models. *Quat. Int.* **2017**, *453*, 63–73. [[CrossRef](#)]
24. Held, I.M.; Soden, B.J. Robust responses of the hydrological cycle to global warming. *Climate* **2006**, *19*, 5686–5699. [[CrossRef](#)]
25. Yao, Z.J.; Guan, Y.P.; Gao, Y.C. Analysis of Distribution Regulation of Annual Runoff and Affection to Annual Runoff by Human Activity in the Chaobaihe river. *Prog. Geogr.* **2003**, *22*, 599–606.
26. Ma, Z.; Ren, X. Drying Trend over China from 1951 to 2006. *Adv. Clim. Chang. Res.* **2007**, *3*, 195–201.
27. Uniyal, B.; Jha, M.K.; Verma, A.K. Assessing Climate Change Impact on Water Balance Components of a River Basin Using SWAT Model. *Water Resour. Manag.* **2015**, *29*, 4767–4785. [[CrossRef](#)]
28. Wang, J.; Wang, E.; Luo, Q.; Kirby, M. Modelling the sensitivity of wheat growth and water balance to climate change in Southeast Australia. *Clim. Chang.* **2009**, *96*, 79–96. [[CrossRef](#)]
29. Gusev, Y.M.; Nasonova, O.N. Application of a technique for scenario prediction of climate change impact on the water balance components of northern river basins. *J. Hydrol. Hydromech.* **2014**, *3*, 197–208. [[CrossRef](#)]
30. Leta, O.T.; El-Kadi, A.; Dulai, H.; Ghazal, K.A. Assessment of climate change impacts on water balance components of Heeia watershed in Hawaii. *J. Hydrol. Reg. Stud.* **2016**, *8*, 182–197. [[CrossRef](#)]
31. Dar, M.; Aggarwal, R.; Kaur, S. Climate Change Impact on Yield and Water Balance Components in Rice-Wheat Cropping System in Central Punjab, India under RCP 8.5. *J. Agric. Allied Sci.* **2017**, *6*, 1–8.

32. Nouri, M.; Homaei, M.; Bannayan, M.; Hoogenboom, G. Towards modeling soil texture-specific sensitivity of wheat yield and water balance to climatic changes. *Agric. Water Manag.* **2016**, *177*, 248–263. [[CrossRef](#)]
33. Essou, G.R.C.; Sabarly, F.; Lucas-Picher, P.; Brissette, F.; Poulin, A. Can precipitation and temperature from meteorological reanalyses be used for hydrological modeling? *J. Hydrometeorol.* **2016**, *17*, 1929–1950. [[CrossRef](#)]
34. Weedon, G.P.; Gomes, S.; Viterbo, P.; Shuttleworth, W.J.; Blyth, E.; Osterle, H.; Adam, J.C.; Bellouin, N.; Boucher, O.; Best, M. Creation of the WATCH Forcing Data and its use to assess global and regional reference crop evaporation over land during the twentieth century. *J. Hydrometeorol.* **2011**, *12*, 823–848. [[CrossRef](#)]
35. Zhang, K.; Kimball, J.S.; Mu, Q.; Running, S.W. Running. Satellite based analysis of northern ET trends and associated changes in the regional water balance from 1983 to 2005. *J. Hydrol.* **2009**, *379*, 92–110. [[CrossRef](#)]
36. Zhang, K.; Kimball, J.S.; Nemani, R.; Running, S.W. A continuous satellite-derived global record of land surface evapotranspiration from 1983 to 2006. *Water Resour. Res.* **2010**, *46*, W09522. [[CrossRef](#)]
37. Warszawski, L.; Frieler, K.; Huber, V.; Piontet, F.; Serdeczny, O.; Schewe, J. The Inter-Sectoral Impact Model Inter-comparison Project (ISI-MIP): Project framework. *PNAS* **2014**, *111*, 3228–3232. [[CrossRef](#)] [[PubMed](#)]
38. McWeeney, C.F.; Jones, R.G. How representative is the spread of climate projections from the 5 CMIP5 GCMs used in ISI-MIP? *Clim. Serv.* **2016**, *1*, 24–29. [[CrossRef](#)]
39. Moss, R.H.; Edmonds, J.A.; Hibbard, K.A. The next generation of scenarios for climate change research and assessment. *Nature* **2010**, *463*, 747–756. [[CrossRef](#)]
40. Hempel, S.; Frieler, K.; Warszawski, L.; Schewe, J.; Pointek, F. A trend-preserving bias correction – the ISIMIP approach. *Earth Syst. Discuss.* **2013**, *4*, 49–92.
41. Arnold, J.G.; Srinivasan, R.; Muttiah, R.S.; Williams, J.R. Large area hydrologic modeling and assessment. Part I: Model development. *Am. Water Resour. Assoc.* **1998**, *34*, 73–89. [[CrossRef](#)]
42. Neitsch, S.L.; Arnold, J.G.; Kiniry, J.R.; Williams, J.R. *Soil and Water Assessment Tool Theoretical Documentation Version 2009*; Texas Water Resources Institute: College Station, TX, USA, 2011.
43. Nijssen, B.; O'Donnell, G.M.; Hamlet, A.F.; Lettenmaier, D.P. Hydrologic sensitivity of global rivers to climate change. *Clim. Chang.* **2001**, *50*, 143–175. [[CrossRef](#)]
44. A Mishra, J.; Froebrich, P.W.; Gassman, J.R. Evaluation of the SWAT model for assessing sediment control structures in a small watershed in India. *Trans. ASABE* **2007**, *50*, 469–477.
45. Zaman, M.; Anjum, M.N.; Usman, M.; Ahmad, L.; Ullah, S.; Yuan, S.; Liu, S. Enumerating the effects of climate change on water resources using GCM scenarios at the Xin'anjiang watershed, China. *Water* **2018**, *10*, 1296. [[CrossRef](#)]
46. Winchell, M.; Srinivasan, R.; Diluzio, M.; Arnold, J. *User's Guide of ARCSWAT Interface for SWAT2012*; Blackland Research and Extension Center TEXAS Agrilife Research: Temple, TX, USA, 2013.
47. Penman, H.L. Evaporation: An introductory survey. *Netherlands J. Agric. Sci.* **1956**, *4*, 7–29.
48. USDA-Soil Conservation Service. *National Engineering Handbook, Hydrology Section 4. Chapters 4-10*; USDA-Soil Conservation Service: Washington, DC, USA, 1972.
49. Cunge, J.A. On the subject of a flood propagation method (Muskingum method). *Hydraul. Res.* **1969**, *7*, 205–230. [[CrossRef](#)]
50. Morris, M.D. Factorial sampling plans for preliminary computational experiments. *Technometrics* **1991**, *33*, 161–174.
51. Abbaspour, K.C.; Yang, J.; Maximov, I.; Siber, R.; Bogner, K.; Mieleitner, J.; Zobrist, J.; Srinivasan, R. Modelling hydrology and water quality in the pre-alpine/alpine Thur watershed using SWAT. *J. Hydrol.* **2007**, *333*, 413–430. [[CrossRef](#)]
52. Nash, J.E.; Sutcliffe, J.V. River flow forecasting through conceptual models part I—A discussion of principles. *J. Hydrol.* **1970**, *10*, 282–290.
53. Feng, S.; Fu, Q. Expansion of global drylands under a warming climate. *Atmos. Chem. Phys.* **2013**, *13*, 10081–10094. [[CrossRef](#)]
54. Sloan, P.G.; Moore, I.D. Modelling subsurface stormflow on steeply sloping forested watersheds. *Water Resour. Res.* **1984**, *20*, 1815–1822. [[CrossRef](#)]

